JOC The Journal of Organic Chemistry

Article

pubs.acs.org/joc

Mechanistic Insight on the Diels–Alder Reaction Catalyzed by a Self-Assembled Molecular Capsule

Lina Xu,[†,‡] Weijie Hua,[†] Shugui Hua,[†] Jun Li,[†] and Shuhua Li*[,†]

[†]School of Chemistry and Chemical Engineering, Key Laboratory of Mesoscopic Chemistry of Ministry of Education, Institute of Theoretical and Computational Chemistry, Nanjing University, Nanjing 210093, People's Republic of China

[‡] College of Chemistry and Materials Engineering, Wenzhou University, Wenzhou 325035, People's Republic of China

Supporting Information

ABSTRACT: We combined Monte Carlo simulations and density functional theory calculations to study the mechanism of the Diels–Alder reaction of *p*-quinone and cyclohexadiene catalyzed by a self-assembled molecular capsule. Our calculations show that the encapsulation of the reactants into the cage is driven by hydrogen-bonding interactions and $\pi-\pi$ stacking interactions between two reactants and the capsule. The encapsulated Diels–Alder reaction at different locations inside the capsule may have quite different reactivity due to different guest–host interactions. A comparison of the free energy profiles of the Diels–Alder reaction in the capsule and in the bulk solution reveals that the Diels–Alder reaction in the capsule is accelerated because the host–guest interaction leads to a relatively smaller barrier for the cycloaddition step.

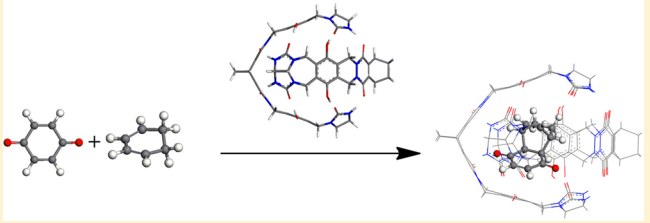

1. INTRODUCTION

The molecular flasks constructed via covalent or noncovalent interactions bear internal cavities that are quite distinct from the external surroundings.[1−8] Within these molecular flasks, the rates of numerous reactions can be significantly accelerated.[9−17] The acceleration effect has been interpreted to be originated from (1) the increase of the concentrations of the reactants inside the flasks,[18−21] (2) the stabilization of the transition state geometry involved in the reaction,[15,16] or (3) the decrease in the entropy of activation for the encapsulated reaction.[22−24] Because of high computational cost, theoretical invesitgations on organic reactions assisted by molecular flasks are still limited, usually based on molecular mechanics (MM) calculations or hybrid quantum mechanics/molecular mechanics (QM/MM) calculations.[25−31] For example, Cantillo and co-workers studied the azide–alkyne cycloaddition assisted by a self-assembled molecular flask with ONIOM (DFT:PM6) calculations.[31] Their calculations show that the rate enhancement of the capsulated reaction may mainly originate from the stabilization of the transition state structure (with respect to the separate reactants).

The Diels–Alder (DA) reaction is one of the most important reactions in organic synthesis. In recent years, chemists have tried to design self-assembled molecular flasks to catalyze this type of reaction. The first classic example is a cagelike, hydrogen-bonded capsule reported by Rebek and co-workers.[18,19] They demonstrated that the DA reaction between *p*-quinone and cyclohexadiene can be accelerated nearly 174-fold within the molecular capsule (as shown in Scheme 1), relative to that in the solvent (*p*-xylene). The proton NMR spectra provide the clear evidence that the DA reaction take places

Scheme 1. Diels–Alder Reaction within the Hydrogen-Bonded Capsule

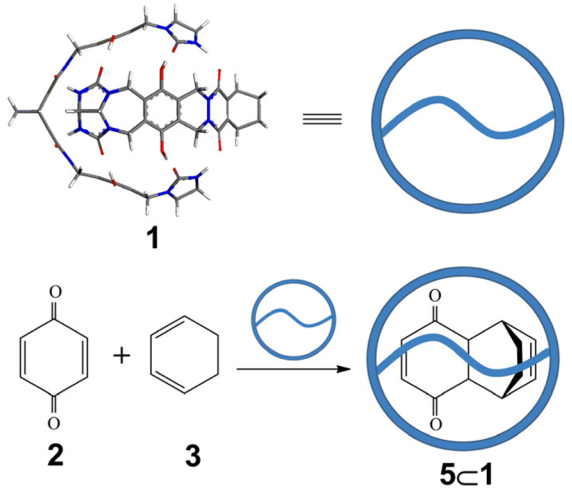

inside the capsule. The experimentalists proposed that the enhanced concentration of the reactants inside the capsule may be responsible for the accelerating effect of encapsulation.

In this work, we investigate the mechanistic details of the encapsulated DA reaction between *p*-quinone and cyclohexadiene at the full quantum mechanical level. We are interested in two key issues: (1) the possible structures of the capsulated reactants, transition states, and products and (2) the

Received: January 10, 2013
Published: March 31, 2013

Table 1. Binding Gibbs Free Energies (kcal/mol) between Separate Reactants or Products and the Capsule along Seven Pathways of the Encapsulated Diels–Alder Reaction in the Solvent

species	path 1	path 2	path 3	path 4	path 5	path 6	path 7
4-X⊂1	−11.1	−9.5	−9.4	−8.6	−8.2	−5.8	−4.7
5-X⊂1	−12.7	−10.8	−13.2	−11.2	−12.5	−10.9	−3.4

Table 2. Relative Gibbs Free Energies (kcal/mol) of Intermediates, Transition States, and Products along Seven Pathways of the Encapsulated Diels–Alder Reaction in the Solvent[a]

species	path 1	path 2	path 3	path 4	path 5	path 6	path 7
4-X⊂1	0.0	1.6	1.7	2.5	2.9	5.3	6.4
TS-X⊂1	19.7	21.2	19.4	22.1	21.7	21.4	23.7
5-X⊂1	−15.9	−14	−16.4	−13.4	−15.7	−14.1	−6.6

[a]The free energy of the intermediate **4-X⊂1** along path 1 is taken as zero.

effect of the host–guest interaction on the free energy profile of the DA reaction. Since the host–guest complex may exist in numerous conformers, we have employed Monte Carlo (MC) simulations to search for several low-energy conformers. With initial structures obtained, we have optimized encapsulated intermediates, transition states, and products along the reaction coordinate with full system density functional theory calculations. The present study reveals that the DA reaction in the capsule is accelerated because the host–guest interaction leads to a relatively smaller barrier for the cycloaddition (relative to that in the bulk solvent).

2. COMPUTATIONAL DETAILS

We adopt the following strategy to study the capsulated DA reaction between *p*-quinone and cyclohexadiene. Considering the fact that the reaction may take place in numerous positions inside the capsule, we need to find a variety of low energy conformers of host–guest association complexes.

To determine the possible low energy conformers of the capsulated encounter complex, we first optimize the encounter complex between *p*-quinone and cyclohexadiene at the M06-2X/6-31G** level.[32,33] Then, we put this encounter complex inside the capsule as the seed and carried out a Metropolis Monte Carlo (MC)[34] calculation to generate a large number of low energy conformers in which the relative positions between the encounter complex and the capsule are different (but intrinsic coordinates of this encounter complex are fixed). The energy of the whole inclusion complex is calculated with the general AMBER force field[35] implemented in the AMBER10 package.[36] In reorientating the encounter complex in the cage, the atoms of the cage are also fixed at their positions (the cage structure is optimized at the M06-2X/6-31G** level). In each MC step, a translation or rotation along one of the *X*, *Y*, *Z* axes of the mass center of the encounter complex is performed. The temperature is chosen as T = 300 K, and the maximum allowed translation and rotation tolerances are set as 0.01 Å and 1 rad, respectively. These settings lead to an acceptance ratio of about 0.4. In the MC simulation, 10^6 configurations are explored. We chose 20 conformers with lowest energies as the initial structures for the subsequent quantum mechanical (QM) calculation. With the lowest energy conformer as the reference, other selected conformers are required to have relatively large room-mean-square deviations (RMSD) (larger than 0.50 Å). With this procedure, the selected low-energy structures are expected to have quite different host–guest interaction modes.

After obtaining 20 initial structures of the host–guest association complexes, we then fully optimize these structures with density function theory calculations. The M06-2X functional will be chosen because it can provide reasonable descriptions for the noncovalent interaction between the substrate and the capsule.[32,33] All calculations are performed with the Gaussian09 program.[37] The 6-31G** basis set is used for all atoms of the capsule and the guest. Full geometry optimizations (the coordinates of all atoms are freely optimized) from 20 initial structures of the host–guest association complexes converge to seven unique optimized structures (their symmetry-equivalent structures are excluded). For each encounter complex, we can easily locate the corresponding encapsulated transition state and the product inside the capsule. For each stationary point, we have performed a vibrational frequency calculation to verify whether it is a minimum or a transition state and obtain its Gibbs free energy at 298.15 K and 1 atm.

Furthermore, for each stationary point we have performed a single-point M06-2X/cc-pVTZ calculation at the optimized geometry described above to get a more accurate electronic energy. The sum of the obtained electronic energy and the thermal free energy obtained with the 6-31G** basis set is taken as the free energy data for each species in gas phase. The polarizable continuum model (PCM)[38−41] is employed to calculate the solvation free energy for each species in the solvent (*p*-xylene). The sum of the gas-phase free energy and the solvation free energy is taken as the free energy in the solvent.

3. RESULTS AND DISCUSSION

For the DA reaction of *p*-quinone with cyclohexadiene in the capsule, we have investigated the free energy profiles of several pathways. In the following, we will first discuss the site preference of the encapsulated DA reaction and then compare the free energy profile of the encapsulated DA reaction with that of the corresponding DA reaction in the bulk solution. The Gibbs free energies are calculated under conditions (298.15 K and 1 atm) with *p*-xylene-d_{10} as the solvent.

3.1. Site Preference of the Encapsulated DA Reaction.

When both *p*-quinone **2** and cyclohexadiene **3** are added to a solution of the dimeric capsule **1**, the reactants are quickly encapsulated into the capsule to form an association complex, as revealed from the experimental study.[18,19] In fact, the association complex may exist in various conformers. We have located several low-energy conformers for the association complex. For each conformer, we have determined the corresponding transition state and the encapsulated product. The binding free energies between separate reactants or products and the capsule along seven pathways are listed in Table 1. The relative free energies of these stationary points along seven pathways (relative to the free energy of the most stable association complex **4-1⊂1**) are listed in Table 2 for comparison. For two pathways, we have displayed the structures of stationary points in Figure 1 (the structures of stationary points along other pathways are shown in Figure S1 in the Supporting Information). As shown in Table 1, the binding free energies of two reactants (with the capsule) along different pathways vary from −4.7 to −11.1 kcal/mol. Different guest–host association complexes may have quite different free energies, as seen also from Table 2. This result is in accord with the experimental fact that the association complex is formed

dx.doi.org/10.1021/jo4000509 | J. Org. Chem. 2013, 78, 3577−3582

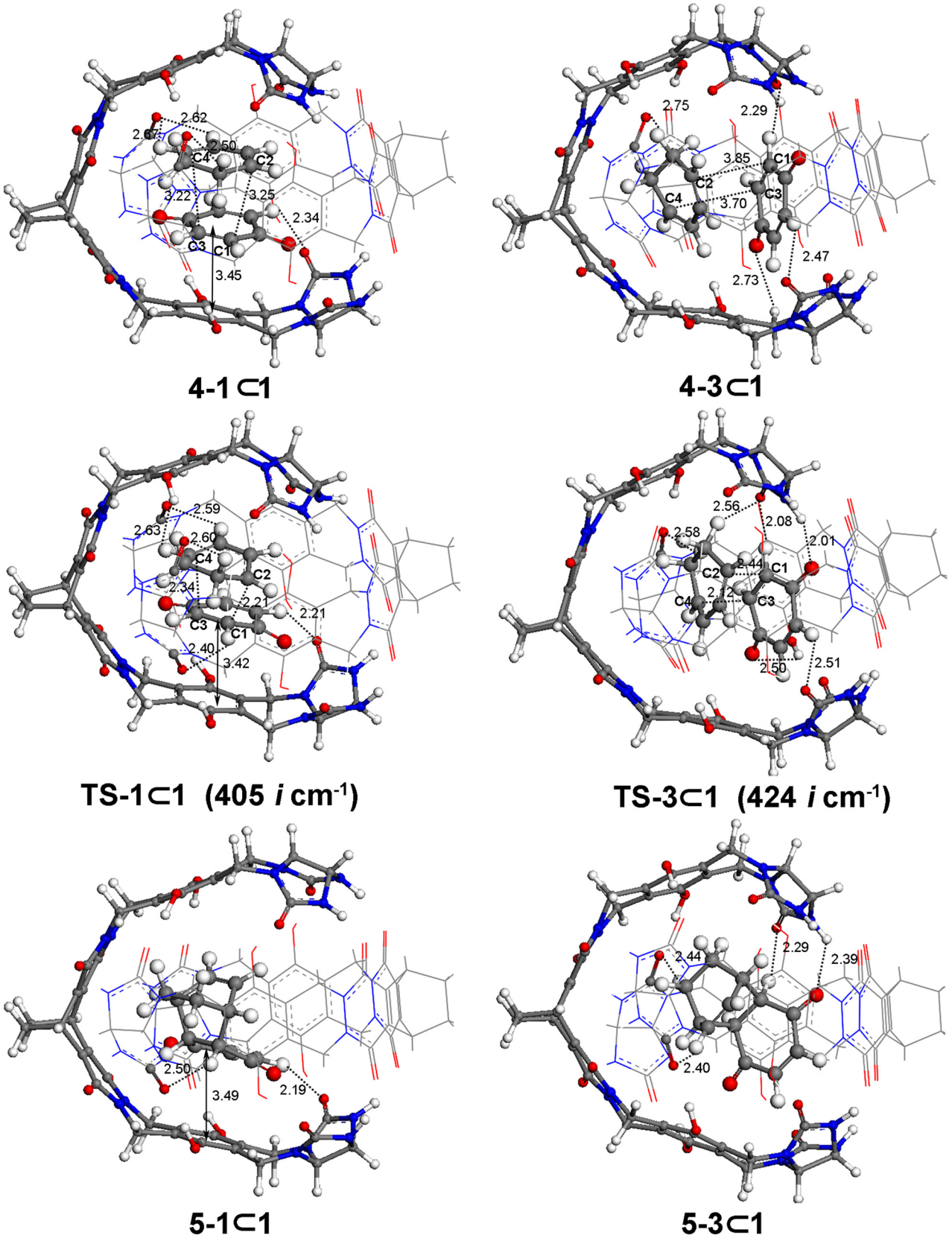

Figure 1. Optimized structures of intermediates, transition states, and products at two different locations inside the capsule.

spontaneously. In the most stable association complex **4-1⊂1**, which is below the separate capsule and two reactants **1**−**3** by 11.1 kcal/mol, two reactants and the capsule form four C−H···O═C hydrogen bonds with distances of 2.34, 2.50, 2.62, and 2.67 Å, respectively. In addition, there exists an intramolecular $\pi-\pi$ stacking interaction between p-quinone and one benzene ring of the cage (with the center-to-center distance of about 3.45 Å). The distances of two C−C bonds

dx.doi.org/10.1021/jo4000509 | J. Org. Chem. 2013, 78, 3577−3582

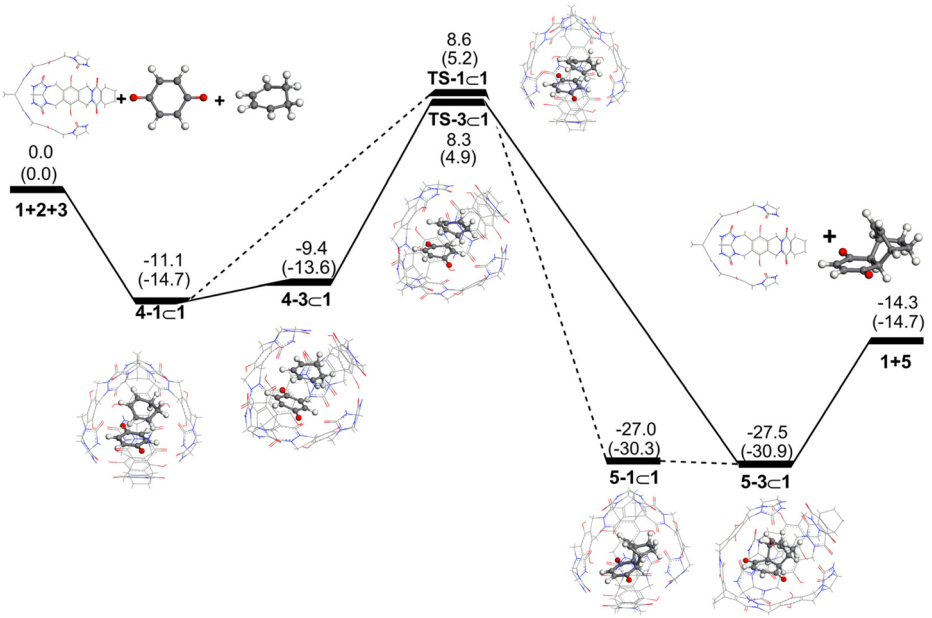

Figure 2. Gibbs free energy profile of the encapsulated DA reaction in the solvent. The energies in the gas phase are also given in parentheses.

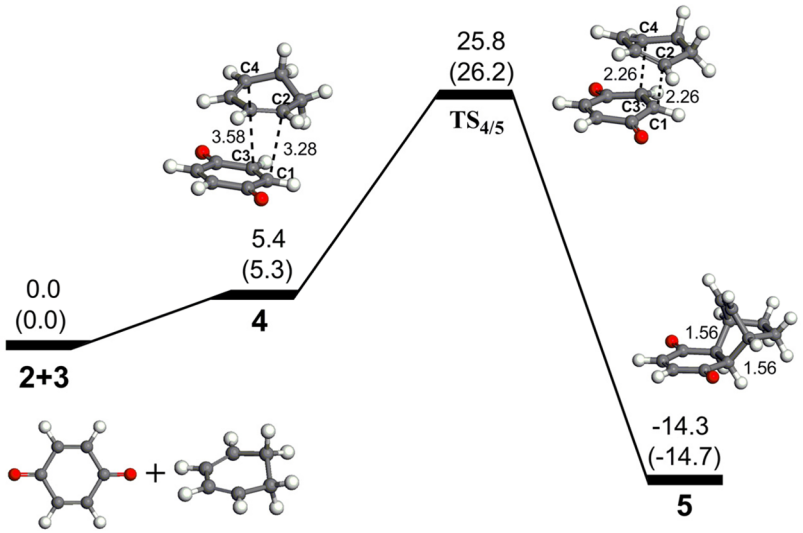

Figure 3. Gibbs free energy profile of the DA reaction in the bulk solution. The energies in the gas phase are also given in parentheses. The distances of two C−C bonds that involve in the cycloaddition reaction are also given.

(C1−C2, C3−C4) that will involve in the subsequent reaction are 3.22 and 3.25 Å, respectively. However, in **4-3⊂1**, there are four C−H...O═C hydrogen bonds between two reactants and the capsule with the distances of 2.29, 2.47, 2.73, and 2.75 Å, respectively. The reactants **2** and **3** inside the capsule **1** are somewhat farther from each other (two C−C bond distances of 3.70 and 3.85 Å, respectively) than they are in **4-1⊂1**. Analyses of various host−guest association complexes show that the association complexes are mainly stabilized by hydrogen bond interactions and $\pi-\pi$ stacking between two reactants and the capsule. The stronger guest−host interaction leads to the more stable association complex.

On the other hand, for various transition states along seven pathways, we notice that **TS-3⊂1** has the lowest free energy, 0.3 kcal/mol lower than **TS-1⊂1**. Inspection of their optimized structures show that **TS-3⊂1** is stabilized by one N−H···O═C, one O−H...O═C, and four C−H···O═C hydrogen bonds (between *p*-quinone, cyclohexadiene, and the capsule's wall), while **TS-1⊂1** is stabilized by an intramolecular $\pi-\pi$ stacking interaction between *p*-quinone and one benzene ring of the cage (with the center-to-center distance of about 3.42 Å) and five C−H···O═C hydrogen bonds. If the encapsulated transition state is less stabilized by the guest−host interaction, the corresponding transition state may be significantly higher in free energy than the lowest transition state **TS-3⊂1**. For example, **TS-7⊂1** is above **TS-3⊂1** by 4.3 kcal/mol (only two C−H···O═C hydrogen bonds exist in **TS-7⊂1**). In addition, we can find that various products have similar binding free energies (except **5-7⊂1**). This is because the compact product can only bind to a small region of the capsule's wall, while the loosely bound association complex and transition state can bind to a much larger region of the capsule's wall.

Let us analyze the reaction barriers of the studied DA reaction at different locations inside the capsule. It can be seen

dx.doi.org/10.1021/jo4000509 | *J. Org. Chem.* 2013, 78, 3577−3582

from Table 2 that the free energy barrier along different pathways varies from 19.4 to 23.7 kcal/mol (with respect to the most stable association complex **4-1⊂1**). For example, the pathway 1 (from **4-1⊂1** to **TS-1⊂1**) has a free energy barrier of 19.7 kcal/mol. For pathway 3, the direct barrier from **4-3⊂1** to **TS-3⊂1** is 17.7 kcal/mol. However, since **4-3⊂1** is less stable than **4-1⊂1** by 1.7 kcal/mol, the overall barrier of **TS-3⊂1** (relative to **4-1⊂1**) is 19.4 kcal/mol. We note that for some pathways, the guest−host interaction stabilizes the "preorganized" intermediate with respect to the transition state, while in other cases, the guest−host interaction destabilizes the "preorganized" intermediate. Hence, the encapsulated DA reaction at different locations may have quite different reactivity, due to different guest−host interactions. To conclude, the encapsulated DA reaction is most likely to proceed via the following steps. The first step is to form the association complex **4-1⊂1**, which has the lowest free energy among various association complexes. Then, this association complex may readily convert into **4-3⊂1**. Since the interconversion between these two isomers only involves the reorientiation of two reactants inside the capsule, this transformation may have a relatively low barrier, compared to the subsequent cycloaddition step. Next, the intermediate **4-3⊂1** undergoes the cycloaddition via **TS-3⊂1** to generate the encapsulated product **5-3⊂1**, which is the most stable product complex. Finally, the product will be released from the capsule. The whole pathway for the encapsulated DA reaction is schematically shown in Figure 2. The overall reaction is exothermic by 14.3 kcal/mol. The rate-determining step on the whole pathway is the cycloaddition with a barrier of 19.4 kcal/mol.

3.2. Comparison of the DA Reaction in the Capsule and the Bulk solution. To understand what factors accelerate the DA reaction within the capsule, we have investigated the free energy profile of the DA reaction between *p*-quinone and cyclohexadiene in the bulk solvent (*p*-xylene-d_{10}). The calculated results are presented in Figure 3. First, these two reactants would also form an encounter complex **4**. In **4**, the distances of two C−C bonds (C1−C2, C3−C4) that will be formed in the cycloaddition step are 3.28 and 3.58 Å, respectively, indicating a strong $\pi-\pi$ stacking interaction between two species. Then, the *endo* product **5** is formed via the transition state $\mathbf{TS}_{4/5}$. The structure of $\mathbf{TS}_{4/5}$ is quite similar to that of the corresponding transition state encapsulated in the capsule described above. Energetically, the encounter complex **4** is thermodynamically less stable than the reactants by 5.4 kcal/mol, and the activation barrier for the cycloaddition reaction is 25.8 kcal/mol (relative to the reactants). This barrier is higher than that of the encapsulated DA reaction by 6.4 kcal/mol. The relatively small free energy barrier for the encapsulated DA reaction provides a qualitative explanation on the acceleration of the DA reaction inside the capsule.

A comparison of the results shown in Figures 2 and 3 can shed light on the factors that contribute to the acceleration of reaction in the capsule. First, the host−guest complex **4-1⊂1** is thermodynamically stable with respect to the separated capsule and the substrate (by 11.1 kcal/mol), while the corresponding encounter complex in the bulk solvent is unstable relative to the separated reactants (by 5.4 kcal/mol). Since the free energy of a species is the sum of the gas-phase free energy and the solvation free energy, we may discuss the contributions of individual terms such as enthalpy, entropy, and solvent effect to the formation of the association complex. For the complex in the capsule, the enthalpic and entropic terms contribute to the free energy change by −41.2 (ΔH) and 26.5 kcal/mol ($-T\Delta S$), respectively, and the solvent effect contributes to 3.6 kcal/mol. In contrast, for the complex in the solution, the corresponding enthalpic and entropic terms are −4.7 and 10.0 kcal/mol, and the solvent effect has a contribution of 0.1 kcal/mol. Clearly, the strong interaction between two reactants and the capsule in the inclusion complex **4-1⊂1** is able to overcome the unfavorable entropic change for the encapsulation process, while the $\pi-\pi$ stacking interaction between two reactants in the complex **4** is not strong enough to overcome the unfavorable entropic change in the association process. From the discussion in the preceding subsection, we can draw the conclusion that the encapsulation of the reactants to form the host−guest complex is driven by hydrogen bonding interaction and $\pi-\pi$ stacking interaction between the reactants and the capsule. On the other hand, the activation barrier of [4 + 2] cycloaddition in the capsule is 19.4 kcal/mol, while the overall barrier in the solution is 25.8 kcal/mol (relative to the separate reactants). One may note that the binding free energy of the two reactants (with the capsule) in the host−guest association complex **4-1⊂1** is −11.1 kcal/mol, and the binding free energy of the transition state with the capsule in the transition complex **TS-3⊂1** is −17.5 kcal/mol. This result shows that the capsule stabilizes the transition state (by 6.4 kcal/mol) more than they do the reactants. To summarize, the acceleration of the DA reaction in the capsule can be ascribed to the fact that the host−guest interaction tends to stabilize the transition state more than the reactants, leading to a relatively smaller reaction barrier.

It should be mentioned that the DA reaction between *p*-quinone and cyclohexadiene may yield both *endo* and *exo* products. Our calculations show that both products have similar thermodynamic stability (their free energies differ from each other by only 0.2 kcal/mol), but the free energy barrier to produce the *exo* product in the bulk solution is 30.4 kcal/mol, higher than that along the *endo* pathway by 4.6 kcal/mol. For the encapsulated DA reaction to produce the *exo* product, we have also obtained the most stable host−guest association complex and the most stable encapsulated transition state. The free energy barrier along the *exo* pathway is 23.2 kcal/mol, being 4.2 kcal/mol higher than that along the *endo* pathway. This result can account well for the fact that only traces of the *exo* product were found.[19]

4. CONCLUSIONS

By combining Monte Carlo simulations and density functional theory calculations, we have studied the mechanism of the Diels−Alder reaction of *p*-quinone and cyclohexadiene in a cagelike, hydrogen-bonded capsule. For a comparison, we have also investigated the free energy profile of the DA reaction between p-quinone and cyclohexadiene in the bulk solvent. One can draw the following conclusions from the present study: (1) The encapsulation of the reactants into the cage is driven by hydrogen-bonding interaction and $\pi-\pi$ stacking interaction between the reactants and the capsule. (2) The encapsulated DA reaction at different locations inside the capsule may have quite different reactivity, due to different guest−host interactions. (3) The DA reaction in the capsule is accelerated (relative to that in the bulk solution) because the host−guest interaction leads to a relatively smaller barrier for the cycloaddition. The present study suggests that the rate of a chemical reaction may be noticeably modulated by the guest−

dx.doi.org/10.1021/jo4000509 | J. Org. Chem. 2013, 78, 3577−3582

host interaction between the substrate and the container. We hope that this study provides some valuable information for chemists to design more effective molecular capsules to modulate a variety of reactions.

■ ASSOCIATED CONTENT

Supporting Information

Optimized geometries of stationary points along the other five pathways inside the capsule; thermodynamic parameters and Cartesian coordinates of all species. This material is available free of charge via the Internet at http://pubs.acs.org/.

■ AUTHOR INFORMATION

Corresponding Author

*E-mail: shuhua@nju.edu.cn.

Notes

The authors declare no competing financial interest.

■ ACKNOWLEDGMENTS

This work was supported by the National Natural Science Foundation of China (Grant Nos. 21073086 and 20833003) and the National Basic Research Program (Grant No. 2011CB808501). Part of the calculations were performed at the High Performance Computing Center of Nanjing University and the Shanghai Supercomputer Center (SSC, China).

■ REFERENCES

(1) Cram, D. J. *Science* **1983**, *219*, 1177−1183.
(2) Cram, D. J. *Nature* **1992**, *356*, 29−36.
(3) Cram, D. J.; Cram, J. M. *Container Molecules and Their Guests*; The Royal Society of Chemistry: Cambridge, 1994.
(4) Conn, M. M.; Rebek, J., Jr. *Chem. Rev.* **1997**, *97*, 1647−1668.
(5) Caulder, D. L.; Raymond, K. N. *Acc. Chem. Res.* **1999**, *32*, 975−982.
(6) Leininger, S.; Olenyuk, B.; Stang, P. J. *Chem. Rev.* **2000**, *100*, 853−908.
(7) Fujita, M.; Tominaga, M.; Hori, A.; Therrien, B. *Acc. Chem. Res.* **2005**, *38*, 371−380.
(8) Vriezema, D. M.; Aragones, M. C.; Elemans, J. A. A. W.; Cornelissen, J. J. L. M.; Rowan, A. E.; Nolte, R. J. M. *Chem. Rev.* **2005**, *105*, 1445−1489.
(9) Mock, W. L.; Irra, T. A.; Wepsiec, J. P.; Manimaran, T. L. *J. Org. Chem.* **1983**, *48*, 3619−3620.
(10) Breslow, R.; Dong, S. D. *Chem. Rev.* **1998**, *98*, 1997−2011.
(11) Richeter, S.; Rebek, J., Jr. *J. Am. Chem. Soc.* **2004**, *126*, 16280−16281.
(12) Pluth, M. D.; Bergman, R. G.; Raymond, K. N. *Science* **2007**, *316*, 85−88.
(13) Yoshizawa, M.; Tamura, M.; Fujita, M. *Science* **2006**, *312*, 251−254.
(14) Koblenz, T. S.; Wassenaar, J.; Reek, J. N. H. *Chem. Soc. Rev.* **2008**, *37*, 247−262.
(15) Yoshizawa, M.; Klosterman, J. K.; Fujita, M. *Angew. Chem., Int. Ed.* **2009**, *48*, 3418−3438.
(16) Brinker, U. H.; Mieusset, J.-L. *Molecular Encapsulation: Organic. Reactions in Constrained Systems*; John Wiley & Sons, Ltd.: Chichester, 2010.
(17) Breiner, B.; Clegg, J. K.; Nitschke, J. R. *Chem. Sci.* **2011**, *2*, 51−56.
(18) Kang, J.; Rebek, J., Jr. *Nature* **1997**, *385*, 50−52.
(19) Kang, J.; Hilmersson, G.; Santamaría, J.; Rebek, J., Jr. *J. Am. Chem. Soc.* **1998**, *120*, 3650−3656.
(20) Chen, J.; Rebek, J., Jr. *Org. Lett.* **2002**, *4*, 327−329.
(21) Kusukawa, T.; Nakai, T.; Okano, T.; Fujita, M. *Chem. Lett.* **2003**, *32*, 284−285.
(22) Fiedler, D.; Leung, D. H.; Bergman, R. G.; Raymond, K. N. *Acc. Chem. Res.* **2005**, *38*, 351−360.
(23) Nishioka, Y.; Yamaguchi, T.; Yoshizawa, M.; Fujita, M. *J. Am. Chem. Soc.* **2007**, *129*, 7000−7001.
(24) Hastings, C. J.; Fiedler, D.; Bergman, R. G.; Raymond, K. N. *J. Am. Chem. Soc.* **2008**, *130*, 10977−10983.
(25) Furuki, T.; Hosokawa, F.; Sakurai, M.; Inoue, Y.; Chûjô, R. *J. Am. Chem. Soc.* **1993**, *115*, 2903−2911.
(26) Beno, B. R.; Sheu, C.; Houk, K. N.; Warmuth, R.; Cram, D. J. *Chem. Commun.* **1998**, 301−302.
(27) Lipkowitz, K. B. *Chem. Rev.* **1998**, *98*, 1829−1873.
(28) Kim, S. P.; Leach, A. G.; Houk, K. N. *J. Org. Chem.* **2002**, *67*, 4250−4260.
(29) Wang, X.; Yang, Z.; Wang, J.; Zhang, J.; Cao, W. *J. Mol. Struct.* **2006**, *766*, 169−175.
(30) Carlqvist, P.; Maseras, F. *Chem. Commun.* **2007**, 748−750.
(31) Cantillo, D.; Ávalos, M.; Babiano, R.; Cintas, P.; Jiménez, J. L.; Palacios, J. C. *Org. Biomol. Chem.* **2011**, *9*, 7638−7642.
(32) Zhao, Y.; Truhlar, D. G. *Theor. Chem. Acc.* **2008**, *120*, 215−241.
(33) Zhao, Y.; Truhlar, D. G. *Acc. Chem. Res.* **2008**, *41*, 157−167.
(34) Metropolis, N.; Rosenbluth, A. W.; Rosenbluth, M. N.; Teller, A. H.; Teller, E. *J. Chem. Phys.* **1953**, *21*, 1087−1092.
(35) Case, D. A.; Darden, T. A.; Cheatham, T. E., III; Simmerling, C. L.; Wang, J.; Duke, R. E.; Luo, R.; Crowley, M.; Walker, R. C.; Zhang, W.; Merz, K. M.; Wang, B.; Hayik, S.; Roitberg, A.; Seabra, G.; Kolossváry, I.; Wong, K. F.; Paesani, F.; Vanicek, J.; Wu, X.; Brozell, S. R.; Steinbrecher, T.; Gohlke, H.; Yang, L.; Tan, C.; Mongan, J.; Hornak, V.; Cui, G.; Mathews, D. H.; Seetin, M. G.; Sagui, C.; Babin, V.; Kollman, P. A. *AMBER 10*, University of California: San Francisco, CA, 2008.
(36) Wang, J.; Wolf, R. M.; Caldwell, J. W.; Kollman, P. A.; Case, D. A. *J. Comput. Chem.* **2004**, *25*, 1157−1174.
(37) Frisch, M. J.; Trucks, G. W.; Schlegel, H. B.; Scuseria, G. E.; Robb, M. A.; Cheeseman, J. R.; Scalmani, G.; Barone, V.; Mennucci, B.; Petersson, G. A.; Nakatsuji, H.; Caricato, M.; Li, X.; Hratchian, H. P.; Izmaylov, A. F.; Bloino, J.; Zheng, G.; Sonnenberg, J. L.; Hada, M.; Ehara, M.; Toyota, K.; Fukuda, R.; Hasegawa, J.; Ishida, M.; Nakajima, T.; Honda, Y.; Kitao, O.; Nakai, H.; Vreven, T.; Montgomery, J. A., Jr.; Peralta, J. E.; Ogliaro, F.; Bearpark, M.; Heyd, J. J.; Brothers, E.; Kudin, K. N.; Staroverov, V. N.; Kobayashi, R.; Normand, J.; Raghavachari, K.; Rendell, A.; Burant, J. C.; Iyengar, S. S.; Tomasi, J.; Cossi, M.; Rega, N.; Millam, N. J.; Klene, M.; Knox, J. E.; Cross, J. B.; Bakken, V.; Adamo, C.; Jaramillo, J.; Gomperts, R.; Stratmann, R. E.; Yazyev, O.; Austin, A. J.; Cammi, R.; Pomelli, C.; Ochterski, J. W.; Martin, R. L.; Morokuma, K.; Zakrzewski, V. G.; Voth, G. A.; Salvador, P.; Dannenberg, J. J.; Dapprich, S.; Daniels, A. D.; Farkas, Ö.; Foresman, J. B.; Ortiz, J. V.; Cioslowski, J.; Fox, D. J. *Gaussian 09*, Revision A.02; Gaussian, Inc.: Wallingford, CT, 2009.
(38) Mennucci, B.; Tomasi, J. *J. Chem. Phys.* **1997**, *106*, 5151−5158.
(39) Cossi, M.; Scalmani, G.; Rega, N.; Barone, V. *J. Chem. Phys.* **2002**, *117*, 43−54.
(40) Tomasi, J.; Mennucci, B.; Cammi, R. *Chem. Rev.* **2005**, *105*, 2999−3093.
(41) Scalmani, G.; Frisch, M. J. *J. Chem. Phys.* **2010**, *132*, 114110−114115.